Energy Proceedings
Vol 59, 2025
ISSN 2004-2965

Molecular Simulation of Water-Based Fracturing Fluid Effects on Methane Adsorption in Shale Nanopores#

ption in Shale Nanopores

Jun Li [1], Zhengfu Ning [2*], Qiang Li [3]

1 Key Laboratory of Petroleum Engineering of the Ministry of Education, China University of Petroleum (Beijing), Beijing 102249, China

2 Key Laboratory of Petroleum Engineering of the Ministry of Education, China University of Petroleum (Beijing), Beijing 102249, China

3 Key Laboratory of Petroleum Engineering of the Ministry of Education, China University of Petroleum (Beijing), Beijing 102249, China

(Corresponding Author: j18765253587@163.com)

ABSTRACT

The retention behavior of water-based fracturing fluids and their impacts on methane adsorption characteristics in deep shale organic nanopores were systematically investigated through molecular simulation. A representative Type II-D kerogen model was employed to examine three prevalent fracturing fluid additives: polyacrylamide (PAM), hydroxypropyl guar gum (GUAR), and cetyltrimethylammonium bromide (CTAB). Complex interactions between fracturing fluids and methane under varying pressure conditions were elucidated through integrated grand canonical Monte Carlo simulations and molecular dynamics simulations, complemented by comprehensive analysis of adsorption isotherms, relative concentration distributions, and Langmuir parameters. A dual adsorption mechanism was demonstrated: while all additives were found to reduce overall methane capacity through pore space occupation (with PAM showing the strongest effect, decreasing Langmuir volume from 24.41 to 20.13 mmol/g), intrinsic methane adsorption capabilities were simultaneously exhibited. Pressure-dependent behavior revealed that low-pressure conditions were dominated by competitive adsorption (GUAR>PAM>CTAB), whereas high-pressure regimes were governed by pore-occupation effects (PAM>CTAB>GUAR). Furthermore, significant differences in additive retention stability were observed, with PAM demonstrating the strongest kerogen adhesion and GUAR exhibiting optimal flowback potential, both of which were directly correlated with their respective interaction energies.

Keywords: Water-based fracturing fluid, Adsorption, Molecular simulation

1. INTRODUCTION

Under the impetus of global carbon neutrality goals, the energy transition process is accelerating, and the strategic importance of unconventional oil and gas resources has become increasingly prominent [1,2]. As a significant unconventional natural gas resource, the efficient development of shale gas plays a crucial role in ensuring energy security. However, shale reservoirs typically possess nanoscale pores and ultra-low permeability characteristics, which severely constrain the commercial development of shale gas [3]. Hydraulic fracturing technology, which significantly enhances reservoir permeability through artificial fractures, has become the core technique for shale gas development.

As a critical component of hydraulic fracturing technology, the performance of fracturing fluids directly affects fracturing effectiveness [4]. Currently, aqueous fracturing fluids dominate shale gas development due to their cost advantages and environmental benefits, primarily including slickwater, guar gum fracturing fluids, and viscoelastic surfactant (VES) fracturing fluids [5]. Notably, although modern fracturing technology has developed comprehensive gel-breaking and flowback processes, field data indicate that 20-35% of fracturing fluids remain persistently retained in the reservoir. These residual fluids ultimately negatively impact shale gas productivity by altering pore structures and affecting methane adsorption/desorption processes [6].

While existing studies have confirmed the phenomenon of fracturing fluid retention and its impact

This is a paper for the 11th Applied Energy Symposium: Low Carbon Cities & Urban Energy Systems (CUE2025), July 18-22, 2024, Kitakyushu, Japan.

on productivity, most research has been limited to macroscopic experimental observations, leaving significant gaps in understanding the microscopic interaction mechanisms. Molecular simulation technology can overcome the limitations of experimental scales and reveal the interaction mechanisms between residual fracturing fluid components and shale organic matter at the molecular level [7-9]. Based on this, this study employs Type II-D kerogen to construct a nano-slit pore model, combined with grand canonical Monte Carlo (GCMC) simulation methods, to systematically investigate the influence of fracturing fluid-kerogen interfacial interactions on methane adsorption behavior. This research not only provides theoretical foundations for clarifying fracturing fluid damage mechanisms but also offers important scientific guidance for optimizing fracturing fluid systems and improving shale gas recovery.

2. METHODOLOGY

2.1 Model construction

This study adopted the Type II-D kerogen molecular topology (chemical formula: $C_{175}H_{102}O_9N_4S_2$) proposed by Ungerer et al. as the modeling foundation [10]. Under the COMPASS II force field, we first performed geometric optimization of the initial molecular structure, followed by 10 cycles of annealing treatment between 300-1000 K to eliminate local energy minima. An initial unit cell model (density 0.1 g/cm^3) containing six optimized kerogen molecules was constructed using the amorphous cell module. Multistage molecular dynamics simulations were conducted for structural relaxation [11]: initial 200 ps relaxation at 1000 K in NVT ensemble, followed by sequential relaxation in NPT ensemble at 900 K, 700 K, 500 K, and 403.15 K (300 ps for each stage). The final stable 3D molecular structure with a density of 1.267 g/cm^3 was used to build a 2×2×1 supercell model, forming a slit-pore structure by adding a 20 Å vacuum layer, as shown in Fig. 1.

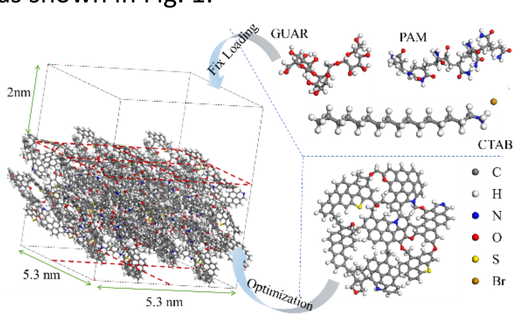

Fig. 1 Model optimization and construction

For the aqueous fracturing fluid system, we focused on three representative additives: polyacrylamide (PAM), hydroxypropyl guar gum (GUAR), and cetyltrimethylammonium bromide (CTAB) [12]. As a friction reducer in slickwater systems, PAM achieves drag reduction primarily through turbulence field regulation. Considering computational limitations for actual polymerization degrees (10^5-10^6), we simplified its polymerization degree to 10 repeating units. Hydroxypropyl guar gum forms 3D network colloidal structures with crosslinkers but undergoes significant degradation after gel breaking, thus its monomer molecule was used to represent degradation products in broken fluids. CTAB, as the main component of viscoelastic surfactant (VES) fracturing fluids, forms viscoelastic structures through micelle entanglement. Since its gel-breaking process only involves physical structural changes without chemical alteration, intact CTAB molecules were directly employed in simulations. These three additives exhibit distinct differences in molecular structures and working mechanisms, which will lead to different impacts on methane adsorption behavior in subsequent simulations.

2.2 Simulation details

This study employed the Sorption module in Materials Studio software to investigate methane adsorption behavior in kerogen slit pores under different fracturing fluid systems. The COMPASS II force field was selected for the simulations, which has demonstrated reliable accuracy and broad applicability in describing shale gas adsorption behavior [13-15]. To accurately simulate the retention effect of fracturing fluids in reservoirs, we first implemented pre-adsorption of fracturing fluid molecules in kerogen slit pores using the Fix Loading task. Three concentration gradients (5, 10, and 15 fracturing fluid molecules) were established to systematically examine the influence of residual fracturing fluid content on methane adsorption mechanisms.

The simulation temperature was strictly maintained at 403.15 K (130 °C), consistent with typical deep shale reservoir conditions. Temperature control was achieved using the Nose-Hoover thermostat method, which effectively maintains thermodynamic equilibrium of the system. Each simulation system underwent an equilibration phase of $1×10^5$ steps to ensure system stabilization, followed by a production phase of $1×10^6$ steps for data collection and analysis [16].

The adsorption study employed 10 characteristic pressure points (1, 3, 6, 9, 12, 15, 20, 30, 40, and 60 MPa) for constant-pressure adsorption simulations. These pressure points, implemented through the Fix Pressure task, cover the complete pressure range from low to high pressure, enabling comprehensive characterization of the entire adsorption process transition from adsorption-dominated to pore-filling-dominated mechanisms. All constant-pressure adsorption simulations maintained the same force field parameters and temperature control methods as the pre-adsorption stage to ensure result consistency and comparability. Throughout the simulations, rigorous monitoring of system energy convergence and configuration stability was performed to obtain reliable equilibrium adsorption data.

3. MATERIAL AND METHODS

3.1 Adsorption isotherm

This study systematically analyzed methane adsorption behavior in kerogen slit pores under different systems using the Langmuir model. The Langmuir model is expressed as Equation (1) [17,18]:

$$V = \frac{V_L P}{P_L + P} \quad (1)$$

where V represents methane adsorption capacity, mmol/g; V_L denotes Langmuir volume, mmol/g, which is the maximum methane adsorption capacity when equilibrium pressure approaches infinity; P is equilibrium pressure, MPa; and P_L represents Langmuir pressure, MPa, corresponding to the pressure at which adsorption reaches half of the maximum capacity.

The methane adsorption behavior in kerogen slit pores exhibited distinct pressure-dependent characteristics. Systematic analysis of adsorption probability distribution (Fig. 2) revealed that under low-pressure conditions, methane molecules preferentially accumulated in high-energy adsorption sites within the kerogen matrix. These sites primarily consist of oxygen-containing functional groups (e.g., carboxyl and hydroxyl groups) and aromatic ring structures, which possess high surface adsorption potential.

As system pressure gradually increased to moderate ranges, the high-energy adsorption sites became saturated, and methane molecules began to diffuse and distribute to secondary adsorption sites with relatively lower adsorption potential. When pressure continued to increase further, a significant transition in adsorption mechanism occurred, shifting from surface adsorption-dominated to pore space filling-dominated adsorption mode.

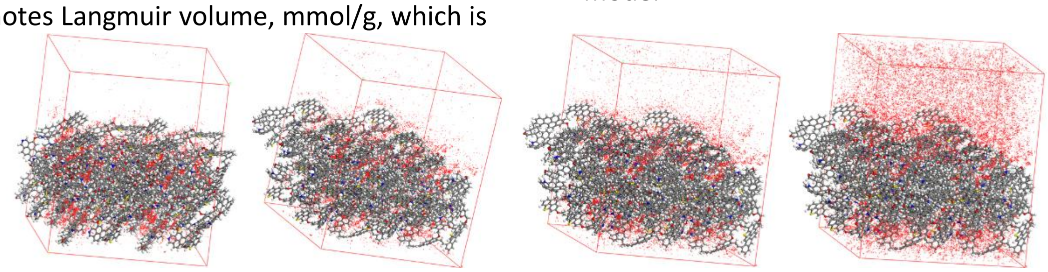

1 MPa 12MPa 20MPa 40MPa

Fig. 2 Variation characteristics of methane adsorption probability with pressure

The study on the influence of different fracturing fluid systems on methane adsorption behavior (Fig. 3) revealed that the methane adsorption isotherm in the pure kerogen system exhibited typical Langmuir-type characteristics: rapid adsorption increase in the low-pressure region, slowed growth rate in the medium-pressure region, and gradual approach to adsorption saturation in the high-pressure region. This nonlinear adsorption feature closely correlates with the progressive occupation of multilevel adsorption sites in shale nanopores. Notably, the introduction of fracturing fluid systems significantly altered this adsorption behavior pattern. Compared with the pure kerogen system, methane adsorption capacity generally decreased in systems containing fracturing fluids, with polyacrylamide (PAM) and cetyltrimethylammonium bromide (CTAB)

systems showing the most pronounced effects.

It is noteworthy that while fracturing fluid systems inhibit methane adsorption, they themselves demonstrate certain methane adsorption capabilities. As shown in Fig. 3, at low-pressure stages, additives primarily affect methane adsorption behavior through competitive adsorption sites, with the guar gum system showing the most significant enhancement effect, following the order: Guar gum > PAM > CTAB. This phenomenon originates from the weak hydrogen bonding between hydroxyl functional groups in guar gum molecules and methane molecules, which facilitates initial methane adsorption under low-pressure conditions.

As pressure increases to high-pressure stages, fracturing fluid systems exhibit completely different mechanisms of action. Although the introduction of fracturing fluids generally reduces methane adsorption capacity in kerogen, localized methane enrichment can still be observed in regions where fracturing fluid molecules aggregate. This dual effect manifests in two aspects: first, the strong interaction between fracturing fluid molecules and kerogen surface preferentially occupies high-energy sites; second, the polar groups and hydrophobic segments of fracturing fluid molecules themselves can provide new adsorption sites for methane.

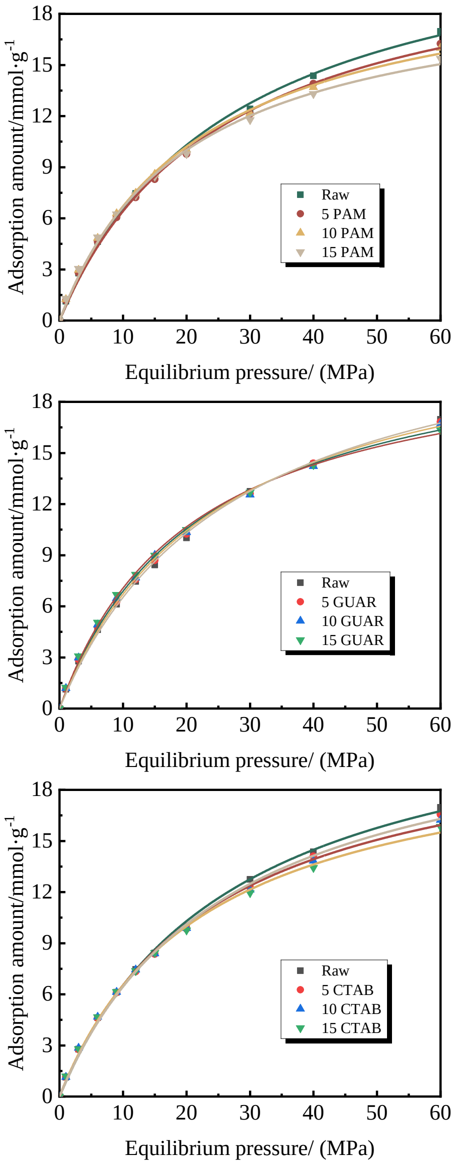

Fig. 3 Methane adsorption isotherms under different fracturing fluid systems

Furthermore, fracturing fluid components physically occupy effective pore space, directly reducing both accessible adsorption sites and free volume for methane molecules, thereby decreasing the overall adsorption capacity of the system. This effect is particularly significant for high-molecular-weight polymers like PAM, whose long-chain structures can substantially alter pore geometry and connectivity, creating more pronounced steric hindrance effects.

3.2 Langmuir parameters

The quantitative analysis results based on the Langmuir adsorption model (Figure 4) clearly demonstrate the differential effects of different types of fracturing fluids on methane adsorption characteristics. The original kerogen system exhibited optimal methane adsorption performance, with a Langmuir volume reaching 24.21 mmol/g. This benchmark value provides an important reference for evaluating the influence of fracturing fluids. After the introduction of fracturing fluids, the adsorption performance of all systems showed varying degrees of decline. Among them, the slickwater system (containing PAM) showed the most significant inhibitory effect, with its Langmuir volume decreasing to 20.13 mmol/g, a reduction of up to 16.9%. In comparison, the effects of guar gum fracturing fluid and clean fracturing fluid (CTAB system) were relatively moderate, with Langmuir volumes decreasing to 22.07 mmol/g and 21.38 mmol/g, corresponding to reductions of 8.8% and 11.7%, respectively.

The changing trend of Langmuir pressure parameters (Fig. 5) further reveals the profound influence of fracturing fluids on adsorption characteristics. The original system had a Langmuir pressure of 27.42 MPa, while after the action of fracturing fluids, this parameter generally showed a downward trend. Specifically, the Langmuir pressure of the slickwater system decreased most significantly to 20.24 MPa, while those of the guar gum fracturing fluid and clean fracturing fluid systems decreased to 21.88 MPa and 22.72 MPa, respectively. This systematic parameter change indicates that fracturing fluid molecules not only reduce the number of effective adsorption sites through physical occupation but, more importantly, alter the energy distribution characteristics of adsorption sites, thereby affecting the equilibrium properties of the entire adsorption system.

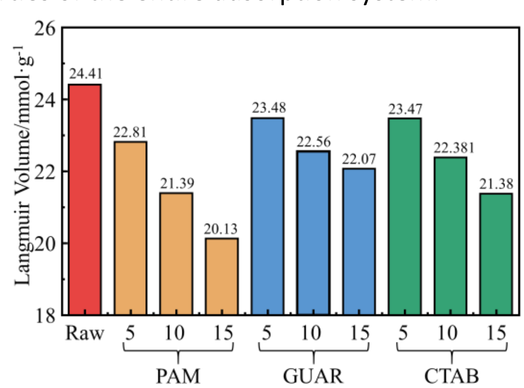

Fig. 4 Langmuir volume of methane adsorption in kerogen under different fracturing fluid systems

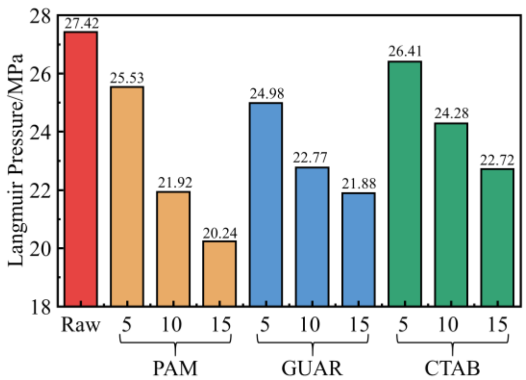

Fig. 5 Langmuir pressure of methane adsorption in kerogen under different fracturing fluid systems

3.3 Relative concentration distribution

By analyzing the relative concentration distribution of methane under different fracturing fluid systems (Fig. 6), distinct spatial distribution characteristics can be observed. In the kerogen pore system, methane molecules primarily accumulate in the surface region of kerogen, a distribution feature particularly pronounced under low-pressure conditions. As system pressure increases, the relative concentration of methane molecules at the kerogen surface gradually decreases, while the methane concentration in the internal pore space shows an increasing trend, reflecting the transition of adsorption mechanisms from surface adsorption to pore filling.

The distribution of fracturing fluid molecules in the pores exhibits obvious aggregation characteristics, forming localized concentration peak regions. In these fracturing fluid aggregation zones, the relative concentration of methane significantly decreases, mainly attributed to two factors: first, the physical occupation effect of fracturing fluid molecules on pore space; second, their competitive occupation of high-energy adsorption sites. Notably, at the edge regions of fracturing fluid aggregation zones, methane concentration shows a slight increase, revealing the secondary adsorption effect of fracturing fluid molecules on methane. This dual-action mechanism indicates that while fracturing fluids generally reduce the methane adsorption capacity of kerogen, their molecular structures themselves possess certain methane adsorption capabilities.

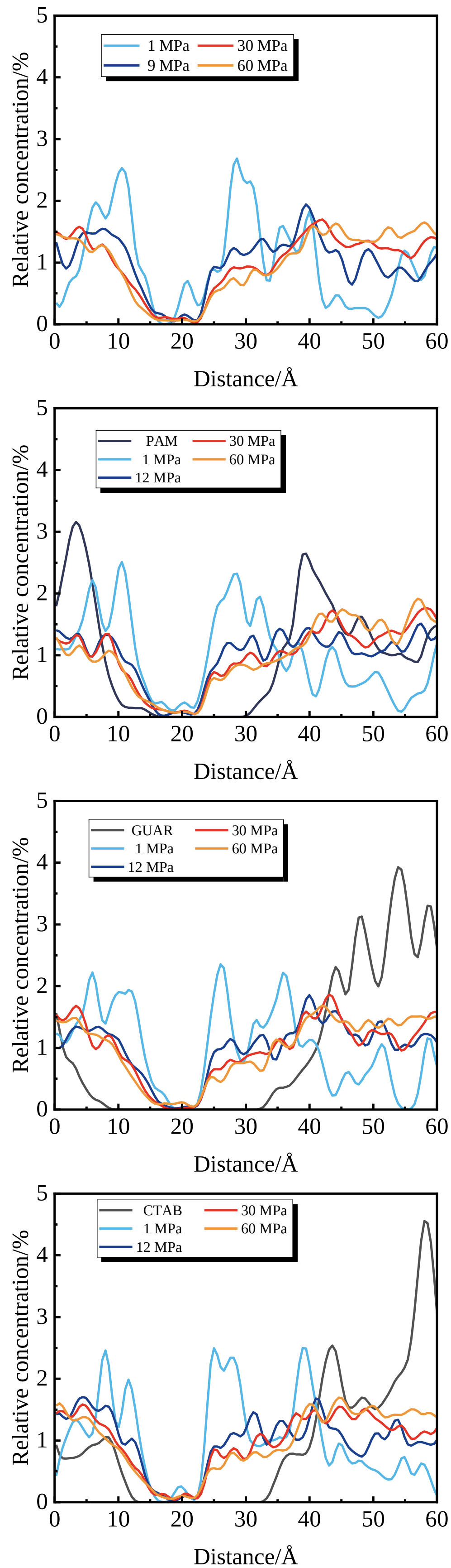

Fig. 6 Distribution characteristics of fracturing fluids and methane in kerogen slit pores under different fracturing fluid systems

Different types of fracturing fluids exhibit distinct distribution characteristics. Due to its long-chain polymer properties, PAM forms relatively dispersed aggregation zones; guar gum molecules demonstrate moderate aggregation due to their polysaccharide structure; while CTAB, as a surfactant, shows the most pronounced localized aggregation characteristics. These differences directly influence the specific patterns of methane concentration distribution in each system, providing a microscopic-level explanation for understanding the impact mechanisms of different fracturing fluids on methane adsorption behavior.

3.4 Adsorption stability

By calculating the interaction energy between fracturing fluids and kerogen (Equation 1), we thoroughly investigated the retention stability mechanism of fracturing fluids in pores [19,20].

$$E_{inter} = E_{total} - (E_{fracturing} + E_{Kerogen}) \quad (2)$$

Where, E_{inter} is the interaction energy between fracturing fluid and kerogen, kcal/mol; E_{total} is the total energy of the adsorption system, kcal/mol; $E_{fracturing}$ is the energy of fracturing fluid, kcal/mol; $E_{kerogen}$ is the energy of the kerogen system, kcal/mol.

The calculation results show that the interaction energies of all systems are negative values, indicating that the adsorption process of fracturing fluid molecules on kerogen surfaces is thermodynamically spontaneous. As the number of fracturing fluid molecules in the system increases, the interaction energy per molecule shows a decreasing trend, reflecting the synergistic effect of intermolecular interactions: when more fracturing fluid molecules are present, the interaction network formed between them enhances the stability of the entire adsorption system.

The three fracturing fluids exhibit significant differences in interaction energy: the PAM system shows the strongest interaction, followed by CTAB, while GUAR is relatively the weakest. This energy difference directly affects their retention characteristics in reservoirs, with PAM being the most difficult to remove due to its strongest interactions. Energy decomposition analysis further reveals that van der Waals forces account for the largest proportion of the total interaction energy and change significantly with increasing molecular number; in comparison, changes in electrostatic interactions are relatively minor. This finding indicates that fracturing fluid molecules primarily bind to kerogen surfaces through van der Waals forces, providing an important theoretical basis for developing targeted fracturing fluid flowback technologies.

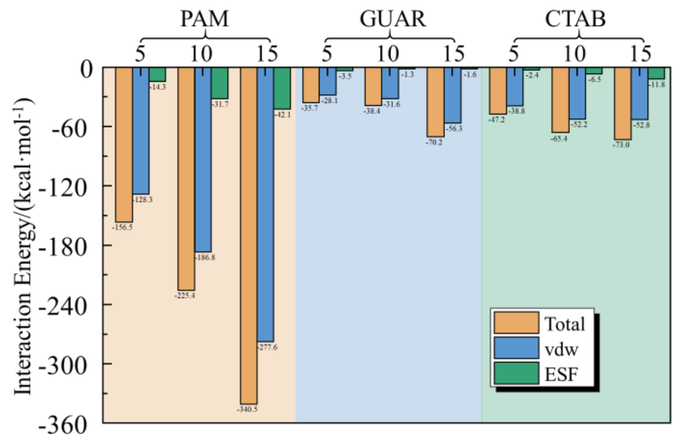

Fig. 7 Interaction forces between different fracturing fluid systems and kerogen

4. DISCUSSION

4.1 Pressure-Dependent Regulation of Adsorption Mechanisms

The study reveals a significant pressure-dependent transition in adsorption mechanisms: competitive adsorption dominates under low-pressure conditions, while pore-occupation effects prevail at high pressures. This finding provides theoretical guidance for fracturing fluid selection under varying reservoir conditions. For instance, in deep high-pressure reservoirs, the pore-blocking effect of PAM becomes the primary limiting factor, suggesting that CTAB or low-molecular-weight fracturing fluids may be more suitable. Conversely, in shallow low-pressure reservoirs, the competitive adsorption characteristics of GUAR could enhance early-stage production capacity due to its hydrogen-bonding interactions with methane.

4.2 Retention Stability and Flowback Strategies for Fracturing Fluids

Interaction energy analysis demonstrates that fracturing fluid retention stability is primarily driven by van der Waals forces (>70% contribution), offering novel insights for optimizing flowback technologies. The high retention energy of PAM explains the poor flowback efficiency observed in field applications of slickwater (Huang et al., 2021). In contrast, the weaker interactions of GUAR suggest that its flowback performance could be further improved through enzyme-based gel-breaker optimization. Future studies may explore the addition of competitive adsorbates (e.g., CO2) or surface modifiers to disrupt van der Waals interactions and enhance the desorption of retained fracturing fluids.

5. CONCLUSIONS

This study systematically investigated the retention behavior of aqueous fracturing fluids in shale nanopores and their impact mechanisms on methane adsorption characteristics through molecular simulation methods, yielding the following main conclusions:

1. Fracturing fluids exhibit a dual mechanism on methane adsorption: while inhibiting methane adsorption through competitive site occupation and pore space blocking, their molecular structures also possess certain methane adsorption capabilities. At low-pressure stages, the guar gum system demonstrates promotional effects on methane adsorption (GUAR > PAM > CTAB), whereas at high-pressure stages, pore-occupation effects dominate, with PAM showing the most significant inhibitory effect (PAM > CTAB > GUAR).

2. Different fracturing fluid types exhibit distinct impacts: the PAM system reduces Langmuir volume from 24.41 to 20.13 mmol/g (17.6% reduction), showing the strongest inhibition; CTAB and guar gum systems decrease to 22.07 and 21.38 mmol/g respectively, with relatively smaller reductions. These differences primarily originate from molecular structure characteristics that determine pore-occupation effects and interaction energy variations.

3. Interaction energy analysis between fracturing fluids and kerogen reveals that the PAM system shows the strongest interaction (PAM > CTAB > GUAR). This energy difference directly determines their retention stability in reservoirs, with PAM being the most difficult to remove and GUAR the easiest to flow back. Microscopic mechanism studies demonstrate that fracturing fluid molecules primarily bind to kerogen through van der Waals forces, and their aggregation patterns and distribution characteristics significantly influence methane adsorption behavior. While creating local concentration depressions, fracturing fluid molecules can also generate secondary methane adsorption in their vicinity.

This research provides theoretical foundations for understanding the microscopic mechanisms of fracturing fluid retention and offers important guidance for optimizing fracturing fluid formulation design.

REFERENCE

[1] Zhao J, Ren L, Lin C, et al. A review of deep and ultra-deep shale gas fracturing in China: Status and directions. Rnew Sust Energ Rev 2025;209:115111.

[2] Mudoi M, Sharma P, Khichi A. A review of gas adsorption on shale and the influencing factors of CH_4 and CO_2 adsorption. J Petrol Sci Eng 2022;217:110897.

[3] Wang E, Zhu H, Yi, et al. Numerical simulation of fracture propagation in high-energy gas fracturing of shale reservoir. Geoenergy Sci Eng 2025;252:213915.

[4] Li J, Ning Z, Wang J, et al. Experimental investigation on the effect of slickwater on methane adsorption/desorption/diffusion and pore structure of shale. Int J Hydrogen Energy 2024;94:871-882.

[5] Huang Q, Liu S, Wang G, et al. Evaluating the changes of sorption and diffusion behaviors of Illinois coal with various water-based fracturing fluid treatments. Fuel 2021;283:118884.

[6] Li J, Huang Q, Wang G, et al. Experimental study of effect of slickwater fracturing on coal pore structure and methane adsorption. Energy 2022;239:122421.

[7] Huang L, Xiao Y, Yang Q, et al. Gas sorption in shale media by molecular simulation: Advances, challenges, and perspectives. Chem Eng J 2024;487:150742.

[8] Lu G, Zou C, Mathews J, et al. Molecular simulation of the potential effects of oxygen functionalities on the adsorption and diffusion of methane in kerogen. Fuel 2025;386:134245.

[9] Li W, Stevens L, Zhang B, et al. Combining molecular simulation and experiment to prove micropore distribution controls methane adsorption in kerogens. Int J Coal Geol 2022;261:104092 .

[10] Ungerer P, Collell J, Yiannourakou M. Molecular modeling of the volumetric and thermodynamic properties of kerogen: influence of organic type and maturity. Energy Fuels 2015;29:91-105.

[11] Si J, Yang X, Li L, et al. Molecular simulation of competitive adsorption of $CO_2/N_2/O_2$ gas in bituminous coal. Colloids Surf A Physicochem Eng Asp 2024;693:134068.

[12] Xue S, Huang Q, Wang G, et al. Experimental study of the influence of water-based fracturing fluids on the pore structure of coal. J Nat Gas Sci Eng 2021;88:103863.

[13] Chen J, Jiang F, Cong Q, et al. Adsorption characteristics of shale gas in organic-inorganic slit pores. Energy 2023;278:127788.

[14] Xu C, Wang W, Wang K, et al. Filling-adsorption mechanism, and diffusive transport characteristics of N_2/CO_2 in coal: Experiment and molecular simulation. Energy 2023;282:128428.

[15] Zhao Y, Wang X, Dong Z, et al. Adsorption behavior of methane in thermally altered coals: A molecular simulation study. Fuel 2025;398:135526.

[16] Babaei S, Ghasemzadeh H, Tesson S, et al. Methane adsorption of nanocomposite shale in the presence of water: Insights from molecular simulations. Chem Eng J 2023;475:146196.

[17] Zhan S, Bao J, Ning S, et al. Effect of surface roughness on methane adsorption in shale organic nanopores from the perspective of molecular simulations. Chem Eng J 2024;498:155322.
[18] Wang L, Liu M, Li J, et al. Investigation of methane adsorption mechanism in Low-Rank bituminous coal considering internal water Distribution: A molecular simulation and experimental study. Chem Eng J 2024;495:153562.
[19] Bai Y, Zhang T, Lin H, et al. Molecular simulation of the effect of anionic surfactant on methane diffusion in coal. Energy 2024;295:131018.
[20] Li S, Yan D, Yan M, et al. Molecular simulation of alkyl glycoside surfactants with different concentrations inhibiting methane diffusion in coal. Energy 2023;263:125771.